Original Article

Investigating the Dosimetric Characteristics of Microbeam Radiation Treatment

Mansour Zabihzadeh[1,2,3], Atefeh Rabiei[2], Hojattollah Shahbazian[3], Sasan Razmjoo[3]

[1]Cancer Research Center, Ahvaz Jundishapur University of Medical Sciences, [2]Department of Medical Physics, School of Medicine, Ahvaz Jundishapur University of Medical Sciences, [3]Department of Clinical Oncology, Golestan Hospital, Ahvaz Jundishapur University of Medical Sciences, Ahvaz, Iran

Abstract

Background: High-radiation therapeutic gain could be achieved by the modern technique of microbeam radiation treatment (MRT). The aim of this study was to investigate the dosimetric properties of MRT. **Methods:** The EGSnrc Monte Carlo (MC) code system was used to transport photons and electrons in MRT. The mono-energetic beams (1 cm × 1 cm array) of 50, 100, and 150 keV and the spectrum photon beam (European Synchrotron Radiation Facility [ESRF]) were modeled to transport through multislit collimators with the aperture's widths of 25 and 50 μm and the center-to-center (c-t-c) distance between two adjacent microbeams (MBs) of 200 μm. The calculated phase spaces at the upper surface of water phantom (1 cm × 1 cm) were implemented in DOSXYZnrc code to calculate the percentage depth dose (PDD), the dose profile curves (in depths of 0–1, 1–2, and 3–4 cm), and the peak-to-valley dose ratios (PVDRs). **Results:** The PDD, dose profile curves, and PVDRs were calculated for different effective parameters. The more flatness of lateral dose profile was obtained for the ESRF spectrum MB. With constant c-t-c distance, an increase in the MB size increased the peak and valley dose; simultaneously, the PVDR was larger for the 25 μm MB (33.5) compared to 50 μm MB (21.9) beam, due to the decreased scattering photons followed to the lower overlapping of the adjacent MBs. An increase in the depth decreased the PVDRs (i.e., 54.9 in depth of 0–1 cm). **Conclusion:** Our MC model of MRT successfully calculated the effect of dosimetric parameters including photon's energy, beam width, and depth to estimate the dose distribution.

Keywords: *Dosimetry, microbeam radiation treatment, Monte Carlo simulation*

Submitted: 29-Jun-2019 **Revision:** 05-Jul-2020 **Accepted:** 11-Jul-2020 **Published:** 30-Jan-2021

Introduction

Radiation therapy can be used to treat many types of cancer either alone or in combination with other treatments. More than half of all cancer patients will require radiation therapy as part of their treatment.[1,2] The main purpose of radiotherapy is to deliver the maximum dose to the tumor and minimum dose to the surrounding healthy tissues. Using the small irradiation fields of modern radiotherapy techniques, such as intensity-modulated radiation therapy,[3] boron neutron capture therapy,[4] and stereotactic radiosurgery,[5,6] reduced the dose delivered to surrounding healthy tissues. This, as a consequence, increases the radiation therapeutic efficacy. Decreasing the field size to microscale and producing the parallel beams compared to those applied in aforementioned techniques are very interested subjects. Moreover, some tumors such as glioblastoma are radioresistant due to low tumor oxygenation (hypoxia), and high dose is needed to ablate them.[7,8] Furthermore, since it promotes cancer cell spreading (invasion) into the healthy brain tissue to evade this adverse microenvironment,[8] delivering high-dose values to target volume in glioma radiotherapy is limited by the high risk of damage to the adjacent healthy tissues, especially in children.[9,10] As known in the literature, the side effects depend on the volume of irradiated brain tissue and the delivered dose values.[11] Hence, decreasing the irradiated volume of the healthy brain tissue could be useful for reducing the side effects. Curtis has shown that complication of healthy tissue to radiation damage induced by microscopically thin beams is negligible.[12] Microbeam radiation therapy (MRT) is based on what is known as the dose–volume effect; the smaller the

How to cite this article: Zabihzadeh M, Rabiei A, Shahbazian H, Razmjoo S. Investigating the dosimetric characteristics of microbeam radiation treatment. J Med Sign Sens 2021;11:45-51.

Address for correspondence:
Dr. Mansour Zabihzadeh, Department of Medical Physics and Department of Clinical Oncology, School of Medicine, Ahvaz Jundishapur University of Medical Sciences, Golestan Blvd., Ahvaz 61357-33118, Iran.
E-mail: manzabih@gmail.com

Access this article online

Website: www.jmssjournal.net

DOI: 10.4103/jmss.JMSS_12_19

Quick Response Code:

field size, the higher the tolerance of the healthy tissue.[12] The cranial malignancies have been reported as an ideal target for MRT. The findings from the literature suggest that head-and-neck sites will be optimal scenarios for MRT.[13,14]

In MRT, using multislit collimator, the highly directional and high-flux synchrotron radiation is built by an array of parallel X-ray microbeams (MBs, from 25 to 75 μm beam width) with a center-to-center (c-t-c) distance of 100–400 μm. The used X-ray energy spectrum from the synchrotron source ranges from 50 to 500 keV.[15-17] Theoretically, the parallel radiation shows a sharply dose drop-off at the edge of each beam-let to limit the delivered dose only to the target volume. High-flux radiation from MRT facility allows delivering of high level of dose (>100 Gy) in a short time that makes it possible to avoid spreading of the dose by tissue movement. The sparing effect of the healthy tissues by different parameter setups for MRT was reported in several preclinical investigations, and some mechanisms such as the poor regenerative capacity of tumoral vessels,[18-24] in-field bystander effects related to cellular migration, and the communication of stress factors between the peak and valley regions,[25,26] were discussed. Experimental dosimetry for MRT has been remained a challenging task due to the need for high spatial resolution dosimeter at high-dose gradient in edges of beamlet and the need for nonsaturated dosimeter to measure high dose delivered inside beamlet.[27-30] Monte Carlo (MC) calculations are not limited by mentioned complications and have been successfully used by some investigators to study different properties of MRT.[15,17,31-34]

Recently, accurate cross-sections and techniques for low-energy electron interactions have been integrated into earlier versions of EGS4 code to improve the accuracy of radiation transport down to 1 keV that is essential for dose calculation at the μm scales in MRT.[35] Instantly, the implementation of some single-particle electron tracking results in better dose calculation as compared to previous techniques of the continuous beam slowing model. Selecting the accurate physical dosimetric properties such as the peak-to-valley dose ratio (PVDR) and the exact value of high dose of several hundred Gray (Gy) depended to X-ray beam spectrum, the c-t-c distance, the irradiation field size, the beam width, the tissue composition, and the depth of tumors. These parameters are essential for a correct dose assessment to establish an optimal treatment plan in the clinical MRT practices. In this study, using the EGSnrc-based MC user codes, the effect of different parameters on dose distribution such as energy of photon, depth, and beam width of MRT was studied.

Materials and Methods

In this study, the radiation transport calculations were carried out using EGSnrc-based MC user codes, 6BEAMnrc, and DOSXYZnrc.[35] Radiation transporting through collimator and dose calculation in phantom were performed using BEAMnrc and DOSXYZnrc, respectively. Considering the energy range of the used photons in MRT, the most significant interaction mechanisms were Compton scattering and photoelectric absorption. Directional bremsstrahlung splitting was used as one of the variance reduction techniques. The MC's parameters are set to ECUT = 521 keV, PCUT = 1 keV, AE = 521 keV, and AP = 1 keV, where ECUT and PCUT are lower energy threshold for electron and photon transport and creation, respectively; the ECUT was set to 50 keV for collimator module to save the calculation time. These low AE and AP values allow simulation of more delta ray and bremsstrahlung production, respectively, which result in more accurate estimation of energy loss straggling. All calculated doses were reported in terms of cGy/incident electron.

Microbeam radiation treatment source model

The lead collimator with a surface of 1 cm × 1 cm, a thickness of 2 cm, 25 μm, or 50 μm a microarray of air apertures, and a fixed c-t-c distance of 200 μm was simulated by component module of MESH to produce array of rectangular planar beams. This arrangement resulted in the MB planar arrays of 50 single beams. The mono-energetic planar beams of 50, 100, and 150 keV were used. The photon source with dimensions of 1 cm × 1 cm was positioned at 5 cm distance from the top surface of the collimator. Furthermore, to mimic a really produced beam by synchrotron, the X-ray spectral distribution was extracted from the ESRF medical beam line (ID17),[36] with an energy bin resolution of 5 keV [Figure 1]. This spectrum with a mean energy of 107 keV contains a small fraction of photons with energies above 300 keV. A total of 109 histories were used to reach a statistical uncertainty better that 0.5%.

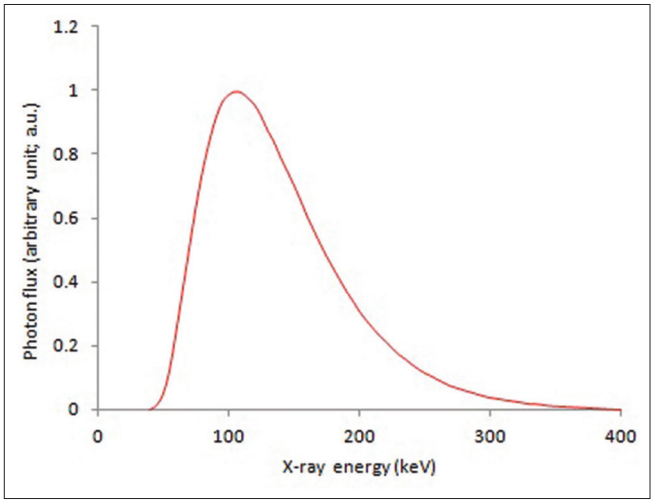

Figure 1: X-ray spectrum of European Synchrotron Radiation Facility ID17 medical beam line, with a 16-mm-thick aluminum filter

Dose calculation

The phase space (PS) file for calculating all dose distributions in the rectangular water phantom with dimensions of 10 cm × 10 cm × 20 cm was generated at the underlined surface of the collimator located 17 cm away from the upper surface of phantom. The PS file contains each particle's type, direction, energy, and position and was used as a source to calculate dose distributions. The PS particles were recycled up to 20 times for each dose calculation. The percentage depth dose (PDD) data were obtained in the central axis of each MB. The voxel dimensions along the central axis were chosen as 1 mm × 1 mm × 2 mm to compromise between resolution needed in the region of high-dose gradient and computational time to obtain the acceptable accuracy. The lateral dose profiles were obtained in three depths 0, 1, and 3 cm in water phantom. These dose values scored in voxels with 1 mm × 2 μm × 1 cm dimensions. All values were normalized to the maximum value on the central axis of MB.

Results

Source model validation

As shown in Figure 2, the calculated depth dose and lateral dose profile were calculated for a planar source using the energy spectrum of ESRF medical beam line (ID17)[36] and compared to the data from Siegbahn *et al*.[37] The difference between our calculated PDD and lateral dose profile with corresponding data reported by Siegbahn *et al*.[37] was <1.5% that is better than 22% reported by Bräuer-Krisch *et al*.[27]

The calculated PDD curves

The calculated depth dose curves for mono-energetic X-ray beams of 50, 100, and 150 keV and X-ray spectrum of ESRF for beam width of 50 μm are shown in Figure 3. All calculated doses were normalized to the maximum dose of 150 keV beam to distinguish low-level discrepancies, especially in the valley region. In Table 1, the percentage dose reductions in depth for a beam width of 50 μm were compared to the absorbed dose on phantom's surface.

The calculated lateral dose profiles

The vertical axes for some lateral dose profiles are presented on a logarithmic scale to illustrate the difference between the curves. The calculated lateral dose profile for the ESRF ID17 spectrum with c-t-c microbeam spacing of 200 μm and microbeam width of 25 μm was depicted in Figure 4. Figure 4a and b shows the calculated lateral dose profiles for seven arrays of microbeams and the central microbeam array, respectively.

To investigate the effect of beam's energy on the lateral dose distribution, the lateral dose profiles are investigated and depicted in Figure 5.

Variation of lateral absorbed dose profiles with depths is evaluated and shown in Figure 6.

The effect of different beam widths (25 and 50 μm) on dose distribution is calculated and presented in Figure 7.

The calculated PVDRs for 1 cm × 1 cm field size depended to different studied parameters of MRT are summarized in Table 2.

Discussion

As shown in Figure 2, the difference between our calculated PDD and lateral dose profile with corresponding data reported by Siegbahn *et al*.[37] was better than 1.5%.

All calculated PDD curves show the descending trend with depth in the phantom primarily due to the attenuation of primary photons.[33-34,36,37] As can be seen in Table 1, the

Table 1: Percentage dose reduction in depth compared to the absorbed dose on phantom's surface for a beam width of 50 μm

Photon energy (keV)	Depth (cm)	
	4 (%)	7 (%)
50	52.9	75.9
100	43.6	65.9
150	40.0	61.6
ESRF spectrum	40.7	62.1

ESRF – European Synchrotron Radiation Facility

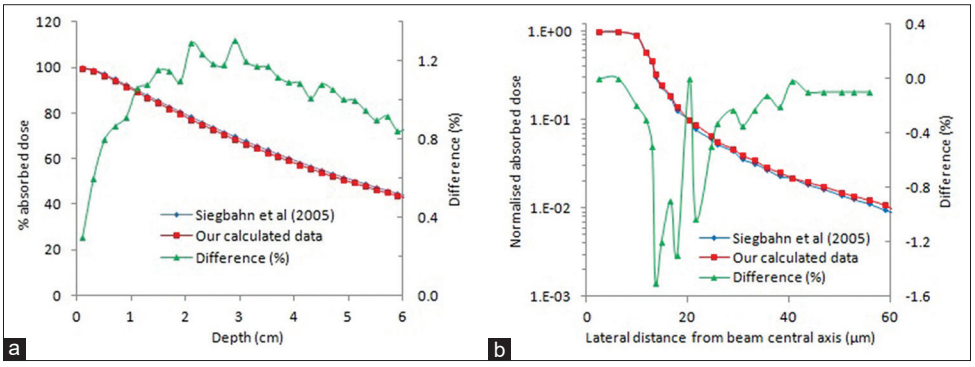

Figure 2: (a) The calculated depth dose and (b) lateral dose profile from full simulated spectrum curves for planar beam. The center-to-center microbeam spacing was 400 *μ*m and the microbeam width was 50 *μ*m

slope of absorbed dose for the lower energy MB is smaller; instantly, for 50 keV beam, delivered dose in the depth of 4 cm was 47.1% of surface dose, while it was 60% for 150 keV beam. This is expected due to the higher range of more energetic photon beam.

As can be seen from Figure 4a and b, the dose is maximal at the center of each MB and decreases toward the edges for each separate MB; the dose flatness on the profile within the central 80% of the beam width is about 10%.

From Figure 5, the dose drops immediately after the edge of the beam in the valley region. This decreased dose is clinically crucial to keep dose delivered to the healthy tissue under tolerances. This deep fall-off of dose is mainly due to lack of primary photons to reach the valley regions which are located in the shadow of lead blocks of collimator. An increase in the energy of photons increases the level of dose in the peak region and at closer distances from beam's edge and also decreases the gradient of dose fall-off, predominately due to electrons from the Compton scattering. For farther distances (>22 μm), the absorbed dose of the ESRF X-ray spectrum is higher than the dose resulted from the higher monochromatic MB of 150 keV. This could be explained by the fact that the ESRF X-ray spectrum includes no negligible contribution of photons with energy higher than 150 keV to produce more scattered photons into the valley region at farther distances. The Compton scattering and photoelectric effect have an opposite behavior at different energies. Consequently, a combination of the two following mechanisms determine absorbed dose in the valley region: (1) the electrons resulting from the Compton scattering deposit their energy in the closer distances from the beam edge as compared to the electrons from photoelectric effect[36] and (2) an increase in the energy of incident photon increases the probability of Compton scattering while decreases the probability of photoelectric effect. These results were also reported by Slatkin *et al*.,[31] Stepanek *et al*.,[32] Spiga *et al*.,[33] and Siegbahn *et al*.[37] Siegbahn *et al*. studied dosimetric properties of MRT (using the ESRF spectrum and mono-energetic MB of 100 keV) by PENELOPE MC code and MOSFET dosimeters. Their results, after suppressing Compton scattering, showed that the photoelectric effect does not contribute fundamentally to shape the dose profile; however, it has a small contribution at adjacent distance from the beam's edge. Shutdown the transportation of secondary electrons in separate calculations resulted that valley dose was created by electrons scattered from the peak region.

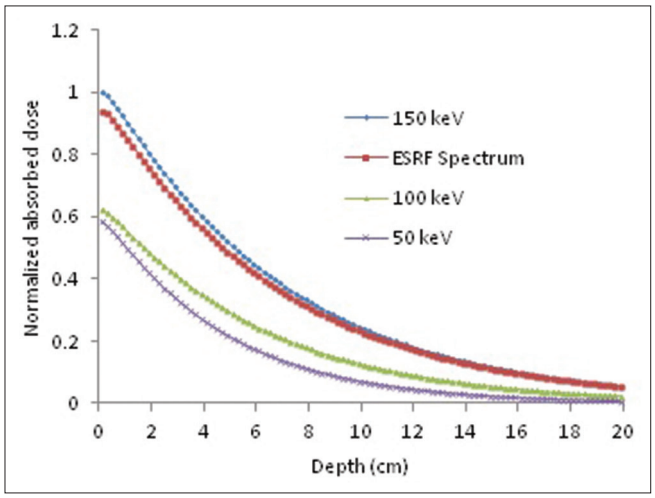

Figure 3: The calculated depth dose curves for 1 cm × 1 cm planar beam at different mono-energetic beams (50, 100, and 150 keV) and European Synchrotron Radiation Facility ID17 spectrum

According to Figure 6a, dose values was decrease with depth. The dose difference between the peak and valley regions becomes smaller by penetrating of photons in deeper depths due to decrease of the primary photon fluence in target volume located at peak regions and increase the fluence of scattered photons received by the valley regions. Considering dose delivery of several hundred Gy in MRT, the increase dose in the valley region from these scattered photons could be a crucial obstacle to obtain the acceptable therapeutic ratio. From Figure 7, although the peak dose is higher for the larger beam's width (50 μm) as a preferred result to deliver high-dose rate, at the same time, the dose

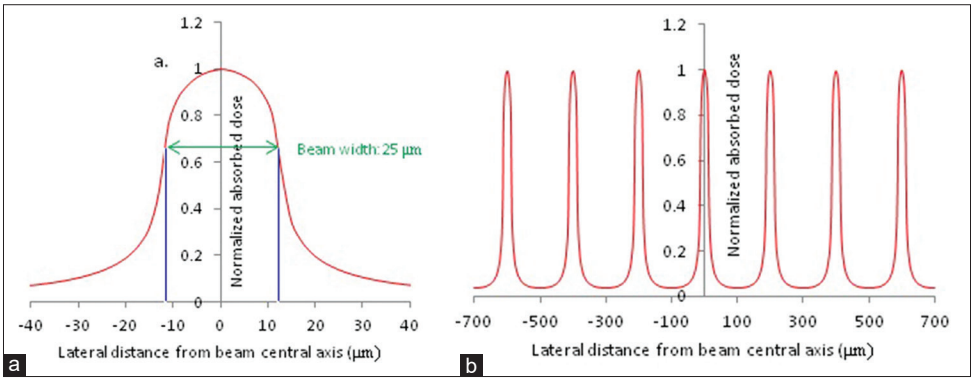

Figure 4: Lateral dose profile for the European Synchrotron Radiation Facility ID17 spectrum for (a) the central microbeam array and for (b) seven arrays of microbeams. The center-to-center microbeam spacing was 200 *μ*m and the microbeam width was 25 *μ*m

absorbed in the valley region would be increased due to the increasing contribution from the scattered MBs.

Conclusion

Our MC model of MRT successfully calculated the dosimetric parameters such as energy of photon, beam width, and depth in phantom to estimate the dose distribution. The PVDR increases with energy of photons and decreases with depth and beam width.

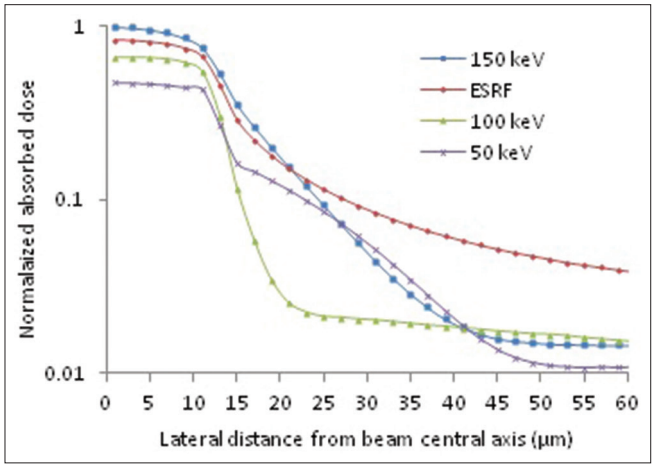

Figure 5: Comparison of the calculated lateral dose profiles for the mono-energetic microplanar beams (50, 100, and 150 keV) and the European Synchrotron Radiation Facility ID17 spectrum X-ray microbeam. The center-to-center of 200 μm and the beam width of 25 μm were used. All calculated doses were normalized to the maximum dose of 150 keV beam

Acknowledgments

This study was a part of MSc thesis of Atefeh Rabiei and supported financially by the research affairs of Ahvaz Jundishapur University of Medical Sciences, Ahvaz, Iran (Grant No: U-95090).

Table 2: Calculated peak-to-valley dose ratios for 1 cm × 1 cm field size of the mono-energetic photons of 50, 100, and 150 keV and European Synchrotron Radiation Facility X-ray spectrum planar microbeams with the fixed center-to-center of 200 μm, beam widths of 25 and 50 μm at depths of 0-1, 1-3, and 3-4 cm inside the water phantom

Microbeam width (μm)	Depth (cm)	Energy of photon (keV)			
		50	100	150	ESRF spectrum
25	0-1	44.4±0.4	54.8±0.5	69.4±0.5	27.9±0.4
	1-2	32.9±0.4	44.0±0.4	54.6±0.4	24.8±0.4
	3-4	28.4±0.4	39.8±0.7	49.4±0.4	23.7±0.4
50	0-1	17.7±0.5	28.9±0.4	42.1±0.4	22.7±0.3
	1-2	14.5±0.4	22.5±0.4	32.8±0.4	19.4±0.3
	3-4	12.8±0.5	20.3±0.4	29.4±0.4	12.9±0.3

ESRF – European Synchrotron Radiation Facility

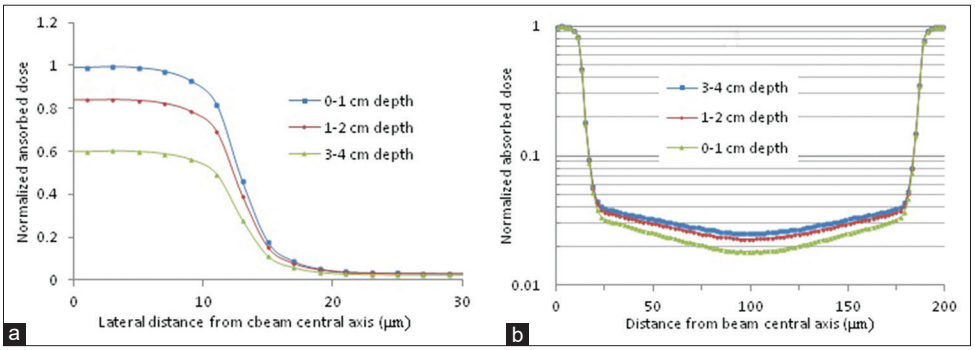

Figure 6: Comparison of the calculated lateral dose profiles in depths of 0–1, 1–2, and 3–4 cm for photon's energy of 100 keV and beam width of 25 *μ*m. Dose distributions were normalized to (a) the maximum value of the profile at depth of 0–1 cm (to highlight difference of peak doses), (b) their maximum values, separately (to highlight difference of valley doses)

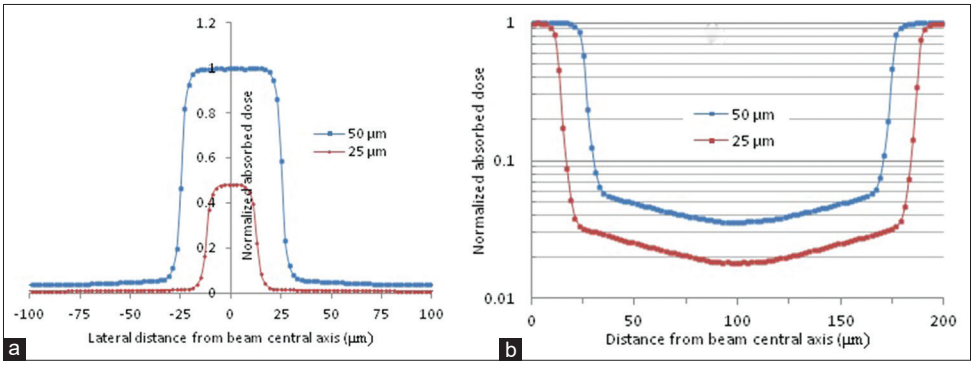

Figure 7: Comparison of the lateral dose profiles on the central axis of the planar microbeam with beam widths of 25 and 50 μm for the photon energy of 100 keV and for the center-to-center of 200 μm. Dose distributions were normalized to (a) the maximum value of dose profile for beam width of 50 *μ*m (to highlight difference of peak doses) and (b) their maximum values, separately (to highlight difference of valley doses)

Financial support and sponsorship

This study was a part of MSc thesis of Atefeh Rabiei and supported financially by the research affairs of Ahvaz Jundishapur University of Medical Sciences, Ahvaz, Iran (Grant No: U-95090).

Conflicts of interest

There are no conflicts of interest.

References

1. Ron E. Ionizing radiation and cancer risk: Evidence from epidemiology. Radiat Res 1998;150:S30-41.
2. Kumar S. Second malignant neoplasms following radiotherapy. Int J Environ Res Public Health 2012;9:4744-59.
3. Cardinale RM, Benedict SH, Wu Q, Zwicker RD, Gaballa HE, Mohan R. A comparison of three stereotactic radiotherapy techniques; ARCS vs. noncoplanar fixed fields vs. intensity modulation. Int J Radiat Oncol Biol Phys 1998;42:431-6.
4. Barth RF, Coderre JA, Vicente MG, Blue TE. Boron neutron capture therapy of cancer: Current status and future prospects. Clin Cancer Res 2005;11:3987-4002.
5. Phillips MH, Stelzer KJ, Griffin TW, Mayberg MR, Winn HR. Stereotactic radiosurgery: A review and comparison of methods. J Clin Oncol 1994;12:1085-99.
6. Zindler JD, Bruynzeel AM, Eekers DB, Hurkmans CW, Swinnen A, Lambin P. Whole brain radiotherapy versus stereotactic radiosurgery for 4-10 brain metastases: A phase III randomised multicentre trial. BMC Cancer 2017;17:500.
7. Monteiro AR, Hill R, Pilkington GJ, Madureira PA. The role of hypoxia in glioblastoma invasion. Cells 2017;6:45.
8. Han X, Xue X, Zhou H, Zhang G. A molecular view of the radioresistance of gliomas. Oncotarget 2017;8:100931-41.
9. Kagan AR, Steckel RJ, Cancilla P, Juillard G, Patin T. The pathogenesis of brain necrosis: Time and dose parameters. Int J Radiat Oncol Biol Phys 1976;1:729-32.
10. Behin A, Hoang-Xuan K, Carpentier AF, Delattre JY. Primary brain tumours in adults. Lancet 2003;361:323-31.
11. Lawrence YR, Li XA, el Naqa I, Hahn CA, Marks LB, Merchant TE, *et al*. Radiation dose-volume effects in the brain. Int J Radiat Oncol Biol Phys 2010;76:S20-7.
12. Curtis HJ. The use of deuteron microbeam for simulating the biological effects of heavy cosmic-ray particles. Radiat Res Suppl 1967;7:250-7.
13. Smyth LM, Day LR, Woodford K, Rogers PA, Crosbie JC, Senthi S. Identifying optimal clinical scenarios for synchrotron microbeam radiation therapy: A treatment planning study. Phys Med 2019;60:111-9.
14. Grotzer MA, Schültke E, Bräuer-Krisch E, Laissue JA. Microbeam radiation therapy: Clinical perspectives. Phys Med 2015;31:564-7.
15. Siegbahn EA, Stepanek J, Bräuer-Krisch E, Bravin A. Determination of dosimetrical quantities used in microbeam radiation therapy (MRT) with Monte Carlo simulations. Med Phys 2006;33:3248-59.
16. Bräuer-Krisch E, Requardt H, Brochard T, Berruyer G, Renier M, Laissue JA, *et al*. New technology enables high precision multislit collimators for microbeam radiation therapy. Rev Sci Instrum 2009;80:074301.
17. Orion I, Rosenfeld AB, Dilmanian FA, Telang F, Ren B, Namito Y. Monte Carlo simulation of dose distributions from a synchrotron-produced microplanar beam array using the EGS4 code system. Phys Med Biol 2000;45:2497-508.
18. Slatkin DN, Spanne P, Dilmanian FA, Gebbers JO, Laissue JA. Subacute neuropathological effects of microplanar beams of X-rays from a synchrotron wiggler. Proc Natl Acad Sci U S A 1995;92:8783-7.
19. Regnard P, Le Duc G, Bräuer-Krisch E, Troprès I, Siegbahn EA, Kusak A, *et al*. Irradiation of intracerebral 9L gliosarcoma by a single array of microplanar X-ray beams from a synchrotron: Balance between curing and sparing. Phys Med Biol 2008;53:861-78.
20. Laissue JA, Lyubimova N, Wagner HP, Archer DW, Slatkin DN, Di Michiel M, *et al*. Microbeam radiation therapy. Denver, Colarado: Proceedings of SPIE-The International Society for Optical Engineering; 3770. p. 38-45.
21. Dilmanian FA, Button TM, Le Duc G, Zhong N, Peña LA, Smith JA, *et al*. Response of rat intracranial 9L gliosarcoma to microbeam radiation therapy. Neuro Oncol 2002;4:26-38.
22. Serduc R, van de Looij Y, Francony G, Verdonck O, van der Sanden B, Laissue J, *et al*. Characterization and quantification of cerebral edema induced by synchrotron X-ray microbeam radiation therapy. Phys Med Biol 2008;53:1153-66.
23. Smilowitz HM, Blattmann H, Bräuer-Krisch E, Bravin A, Di Michiel M, Gebbers JO, *et al*. Synergy of gene-mediated immunoprophylaxis and microbeam radiation therapy for advanced intracerebral rat 9L gliosarcomas. J Neurooncol 2006;78:135-43.
24. Bouchet A, Sakakini N, El Atifi M, Le Clec'h C, Brauer E, Moisan A, *et al*. Early gene expression analysis in 9L orthotopic tumor-bearing rats identifies immune modulation in molecular response to synchrotron microbeam radiation therapy. PLoS One 2013;8:e81874.
25. Crosbie JC, Anderson RL, Rothkamm K, Restall CM, Cann L, Ruwanpura S, *et al*. Tumor cell response to synchrotron microbeam radiation therapy differs markedly from cells in normal tissues. Int J Radiat Oncol Biol Phys 2010;77:886-94.
26. Autsavapromporn N, Suzuki M, Funayama T, Usami N, Plante I, Yokota Y, *et al*. Gap junction communication and the propagation of bystander effects induced by microbeam irradiation in human fibroblast cultures: The impact of radiation quality. Radiat Res 2013;180:367-75.
27. Bräuer-Krisch E, Bravin A, Lerch M, Rosenfeld A, Stepanek J, Di Michiel M, *et al*. MOSFET dosimetry for microbeam radiation therapy at the European Synchrotron Radiation Facility. Med Phys 2003;30:583-9.
28. Archer J, Li E, Davis J, Cameron M, Rosenfeld A, Lerch M. High spatial resolution scintillator dosimetry of synchrotron microbeams. Sci Rep 2019;9:6873.
29. Sharma SD. Challenges of small photon field dosimetry are still challenging. J Med Phys 2014;39:131-2.
30. Bartzsch S, Corde S, Crosbie JC, Day L, Donzelli M, Krisch M, *et al*. Technical advances in x-ray microbeam radiation therapy. Phys Med Biol 2020;65:02TR01.
31. Slatkin DN, Spanne P, Dilmanian FA, Sandborg M. Microbeam radiation therapy. Med Phys 1992;19:1395-400.
32. Stepanek J, Blattmann H, Laissue JA, Lyubimova N, Di Michiel M, Slatkin DN. Physics study of microbeam radiation therapy with PSI-version of Monte Carlo code GEANT as a new computational tool. Med Phys 2000;27:1664-75.
33. Spiga J, Siegbahn EA, Bräuer-Krisch E, Randaccio P, Bravin A. The GEANT4 toolkit for microdosimetry calculations: Application to microbeam radiation therapy (MRT). Med Phys 2007;34:4322-30.
34. Schreiber EC, Chang SX. Monte Carlo simulation of

a compact microbeam radiotherapy system based on carbon nanotube field emission technology. Med Phys 2012;39:4669-78.
35. Kawrakow I. Accurate condensed history Monte Carlo simulation of electron transport. I. EGSnrc, the new EGS4 version. Med Phys 2000;27:485-98.
36. De Felici M, Felici R, Sanchez del Rio M, Ferrero C, Bacarian T, Dilmanian FA. Dose distribution from x-ray microbeam arrays applied to radiation therapy: An EGS4 Monte Carlo study. Med Phys 2005;32:2455-63.
37. Siegbahn E, Bräuer-Krisch E, Stepanek J, Blattmann H, Laissue J, Bravin A. Dosimetric studies of microbeam radiation therapy (MRT) with Monte Carlo simulations. Nucl Instrum Methods Phys Res 2005;548:54-8.

BIOGRAPHIES

Mansour Zabihzadeh received his B.Sc degree in physics in 2000 from Shahid Rajaee University of Karaj, Karaj, Iran; and he obtained his MSc and PhD degree in medical physics from Tehran University of medical Sciences, Tehran, Iran in 2003 and 2009 respectively. He is now an associated professor at Ahvaz Jundishapur University of medical Sciences. His research interests include Radiotherapy, Radiation dosimetry, Medical Imaging and Simulation.

Email: manzabih@gmail.com

Atefeh Rabiei received her B.Sc degree in Physics from University of Arak, Arak, Iran in 2012, and she got her M.Sc from Ahvaz Jundishapur University of medical Sciences in 2018. Her research interests are in the fields of Radiotherapy, Radiation dosimetry and Simulation.

Email: ateferabiei@yahoo.com

Hojattollah Shahbazian received his MD degree from Tehran University of medical Sciences, Tehran, Iran, in 1996 and his Radiotherapy from Shahid Beheshti University of medical Sciences, Tehran, Iran in 2004 He is currently associate professor at Ahvaz Jundishapur University of medical Sciences. His research interest is in the field of Radiation therapy.

Email: hjshahbazian@yahoo.com

Sasan Razmjoo received his MD degree from Ahvaz Jundishapur University of medical Sciences, Ahvaz Iran, in 2004 and his Radiotherapy from Shiraz University of medical Sciences, Tehran, Iran in 2009 He is currently associate professor at Ahvaz Jundishapur University of medical Sciences, His research interests in the field of Radiation therapy.

Email: razmjoo.md@gmail.com